Experimental Study on Microwave Generation due to Merged Instability in F-Band Surface Wave Oscillator*)

Keiichiro RACHI, Kazuo OGURA, Yuta ANNAKA[1)], Mao AOKI and Tsubasa KATO

Graduate School of Science and Technology, Niigata University, Niigata 950-2181, Japan

[1)]*Faculty of Engineering, Niigata University, Niigata 950-2181, Japan*

(Received 1 December 2020 / Accepted 10 January 2021)

A surface wave oscillator (SWO) is driven by an electron beam to generate intense microwaves. The electron beam possesses slow space-charge (SSC) and slow cyclotron (SC) modes that interact with the surface wave leading to microwave generation. The beam current and external magnetic field affect the relationship between SSC and SC modes. The SSC mode gradually approaches the SC mode when the beam current increases. Meanwhile the SC mode gradually approaches the SSC mode when the magnetic field decreases. The two modes merge in a low magnetic field and high beam current. In this work, we experimentally examine the operation of an F-band SWO in the low magnetic field region. The output power decreases with low beam current when magnetic field decreases. Meanwhile, the SWO maintains its power level with high beam current even though the magnetic field decreases to around 0.4 T. The merged instability enables a sustained power level in the low magnetic field region.

Keywords: surface wave oscillator, merged instability, intense terahertz radiation, slow cyclotron instability, Cherenkov instability

DOI: 10.1585/pfr.16.2401028

1. Introduction

A surface wave oscillator (SWO) has been studied as one of high-power microwave and terahertz-wave sources. This device can output a high-power microwave using an interaction between a surface wave and an injected electron beam in an oversized slow-wave structure (SWS) with periodical corrugations [1, 2]. In order to properly propagate electron beam, an external magnetic field is used and its intensity is typically 1 T or less [3]. In Ref. [1], a MW-level terahertz radiation from a Y-band SWO is obtained with 3.1-T magnetic field. A SWO can be a compact device because it requires a lower magnetic field than other electron-beam devices, like a gyrotron that requires 10-T magnetic field or more in the terahertz frequency region [4, 5]. To make the SWO even more compact, we examine intense microwave oscillation in a low magnetic field region.

An electron beam has four modes: fast space charge (FSC) and slow space charge (SSC) modes and fast cyclotron (FC) and SC modes. In general, a SWO generates intense microwaves by using the Cherenkov interaction between the surface wave and the SSC mode. However, a recent numerical study in Ref. [6] indicated the importance of the SC mode. When the magnetic field decreases, the interaction between the surface wave and the SC mode increases and becomes comparable with the Cherenkov interaction. With a sufficiently low magnetic field, the SC mode combines with the Cherenkov mode to form a merged instability. The growth rate of the merged instability is larger than those of the Cherenkov and SC instabilities. Availability of the SC and merged instabilities to terahertz-wave sources is still unclear. And hence operation of SWOs in the low magnetic field region should be studied in more detail.

In this paper, we study intense operation of an F-band SWO in a magnetic field less than 1 T. The beam interactions with the surface wave are examined considering SSC and SC modes. The two modes merge with a sufficiently low magnetic field. We experimentally examine how the merged instability affects the output power of the SWO.

2. Experimental Setup

A schematic diagram of the SWO experiment is shown in Fig. 1. A cathode and the waveguides, including an F-band SWS with a corrugated waveguide, are placed in

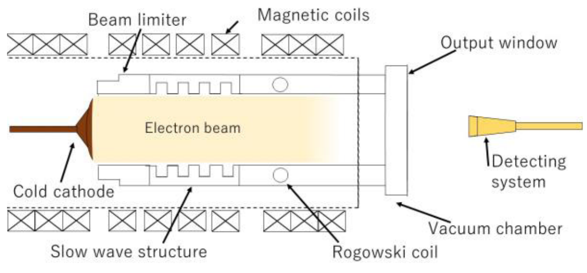

Fig. 1 Schematic diagram of a surface wave oscillator.

author's e-mail: f19c075k@mail.cc.niigata-u.ac.jp

*) This article is based on the presentation at the 29th International Toki Conference on Plasma and Fusion Research (ITC29).

a vacuum chamber with a base pressure of approximately 3 - 5 × 10^{-3} Pa. To generate an annular electron beam, we use a disk-type cold cathode developed for weakly relativistic microwave devices [7]. A hollow beam limiter is placed as an anode in front of the waveguide and has a role to shape the electron beam. The SWS with a rectangularly corrugated waveguide forms a surface wave on the wall surface, which interacts with the electron beam. The size parameters of the SWS are a periodic length $z_0 = 0.5$ mm, a groove length $d = 0.3$ mm, and a groove depth $2h = 0.6$ mm. The diameter of the beam limiter is 29.7 mm, which is the same as the diameter of the F-band SWS. The beam current is measured by a Rogowski coil in the back of the SWS. Magnetic coils provide a magnetic field from 0 to 1 T. A detection system picks up the microwave output using F-band waveguides, whose recommended frequency band is from 90 to 140 GHz.

The disk-type cold cathode is made of oxygen-free copper with a diameter of 29.5 mm. A burn pattern of the beam on thermal paper is shown in Fig. 2 (a). The pattern has a fairly good annular shape with nearly the same outer diameter as that of the beam limiter. The thickness of the pattern is approximately 2 mm. The beam current and voltage are 95 A and 22 kV, respectively. Here, we see the relationship between the beam location and the corrugation. The radial distribution of the surface wave intensity in the SWS can be calculated [3] and is plotted in Fig. 2 (b). In a cylindrical SWS with a period of z_0, the axial electric field E_z is given by

$$E_z = \sum_{p=-\infty}^{\infty} A_p J_m(x_p r) \exp(ik_p z + im\theta - i\omega t), \quad (1)$$

and

$$x_p^2 = \omega^2/c^2 - k_p^2. \quad (2)$$

Here, A_p is the amplitude of J_m, J_m is the m-th order Bessel function of the first-kind, m is an azimuthal mode number, $k_p = k_z + pk_0$, p is the spatial harmonic number, and $k_0 = 2\pi/z_0$ is the corrugation wave number. Focusing on our SWO, the surface wave is much slower than the speed of light $x_p^2 \ll 0$ and for all spatial harmonics. Hence, the surface wave intensity decreases sharply away from the SWS wall. In Fig. 2 (b), the intensity of the surface wave becomes maximum at 14.85 mm which corresponds to the corrugated wall. The intensity decays to almost zero at 14.0 mm from the corrugated wall. The electron beam needs to propagate in the region between 14.0 to 14.85 mm to effectively interact with the surface wave.

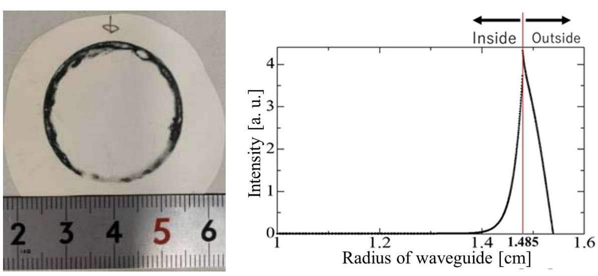

(a) (b)

Fig. 2 (a) Burn pattern of electron beam on thermal paper. (b) Intensity of electric field in the F-band corrugated waveguide. The radius of corrugated wall is 1.485 cm. "Inside" and "Outside" represent the areas inside and outside of the corrugation groove, respectively.

3. Beam Interactions

In this section, beam interactions with the surface wave are examined based on the experimental parameters presented in the previous section. The dispersion characteristics are calculated as shown in Fig. 3, following the numerical method presented in Ref. [6]. The cylindrical waveguide system has transverse electric (TE) and transverse magnetic (TM) modes. Transverse cyclotron perturbations of the electron beam combine the TM and TE modes, even in axisymmetric cases. In Fig. 3, the axisymmetric EH_{01} waveguide mode corresponds to the fundamental TM_{01} in a vacuum case. We assume an annular sheet electron beam with a diameter of 29.5 mm, a current of 150 A, and an energy of 20 keV. The magnetic field is 0.8 T. The space charge modes are given by

$$\omega = vk_z \pm \omega_b/\gamma. \quad (3)$$

The +(−) sign corresponds to the FSC (SSC) mode, and the cyclotron modes are given by

$$\omega = vk_z \pm \omega_c. \quad (4)$$

The +(−) sign corresponds to the FC (SC) mode, which is caused by the normal (anomalous) Doppler effect [8]. Here, ω is the angular frequency of the beam mode, v is the velocity of electron beam, k_z is the axial wave number, ω_b is the plasma angular frequency of the beam, γ is the relativistic factor, and ω_c is the electron cyclotron angular frequency.

In Fig. 3, the EH_{01} waveguide mode interacts with the SSC mode and then the Cherenkov instability occurs. The

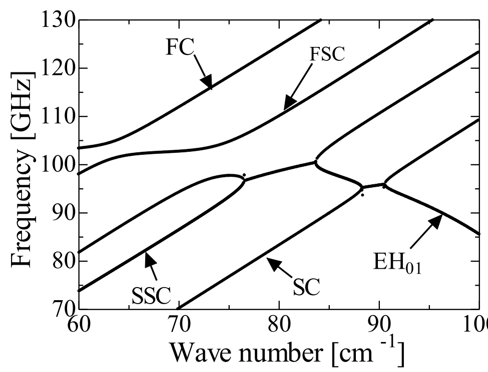

Fig. 3 Dispersion characteristics of the F-band SWO driven by a beam of 150 A and 20 keV. The magnetic field is 0.8 T.

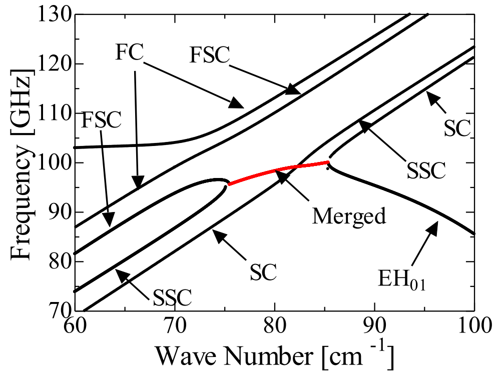

Fig. 4 Dispersion characteristics of the F-band SWO driven by a beam of 150 A and 20 keV. The magnetic field is 0.4 T. In this case, the interchange among beam modes takes place. The beam modes are identified using saddle-point analysis from Ref. [6].

SSC mode is affected by the plasma oscillation of the beam whose angular frequency ω_b is given by

$$\omega_b = \sqrt{n_0 e^2/\varepsilon_0 m_0 \gamma}. \tag{5}$$

Here, n_0 is the electron density of the beam and m_0 is the rest mass of the electron. Moreover, the beam current I_b is expressed as

$$I_b = e n_0 v S_0, \tag{6}$$

where, S_0 is the cross section of the annular electron beam. When the current I_b increases, the electron density n_0 and plasma frequency ω_{pe} also increase. Then, the SSC mode of Eq. (3) approaches the SC mode of Eq. (4). The EH01 waveguide mode interacts with the SC mode and the SC instability occurs.

The cyclotron angular frequency ω_c is given by

$$\omega_c = eB/\gamma m_0. \tag{7}$$

Here, B is the external magnetic field. When magnetic field B decreases, ω_c also decreases and the SC interaction point approaches the Cherenkov interaction point. Figure 4 shows the dispersion relation with a low magnetic field of 0.4 T, which is lower than that of Fig. 3. The SC and SSC modes interact in the same instability of the EH$_{01}$ mode, leading to the merged instability.

Figure 5 (a) shows the dependence of the EH$_{01}$ instabilities on the magnetic field; the beam energy is 20 keV. For the current of 50 A, the Cherenkov and SC instabilities exist separately and merge at 0.3 T. The temporal growth rate of the merged instability is higher than those of the SC and Cherenkov instabilities. When the beam current is increased to 150 A, the growth rates of Cherenkov and SC instabilities increase, and the merged instability occurs at around 0.5 T. This magnetic field increases by increasing the beam current.

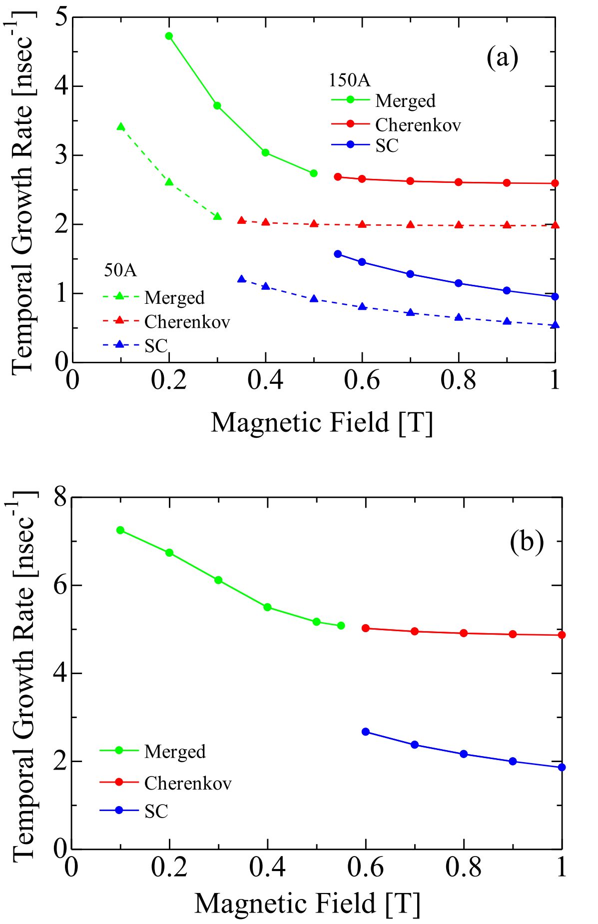

Fig. 5 Magnetic field dependence of the temporal growth ratesof the F-band SWO. (a) The beam energy is 20 A and the currents are 50 A and 150 A. The distance Gbbetween the beam and the SWS inner wall is 0.1 mm. (b) The beam energy and current are 25 keV and 110 A with G_b = 0.01 mm.

4. Experimental Results

Waveforms of measured signals for the F-band SWO are shown in Fig. 6. The microwave signals are received by the F-band horn antenna placed 600 mm away from the output window. After adequate attenuation, the microwave is detected by crystal detectors. In Figs. 7 (a) and (b), the detected power, beam current, and beam voltage are plotted as a function of the magnetic field. The voltage and current vary with time in the experiment and their values at the time of peak radiation are plotted. Here, five shots are measured at each magnetic field and the average values are plotted. For Fig. 7 (a), the average voltage and current are in the range of 15 - 20 kV and 50 - 70 A, respectively. The output power sharply decreases from 0.8 T and no meaningful radiation is detected at fields less than 0.6 T. This power decrease may be caused by a degradation of the electron beam confinement owing to the decreased magnetic field. On the other hand, meaningful radiation is detected down to around 0.4 T in Fig. 7 (b), where the beam current increases. The average voltage and current are in the range of 20 - 26 kV and 100 - 170 A, respectively.

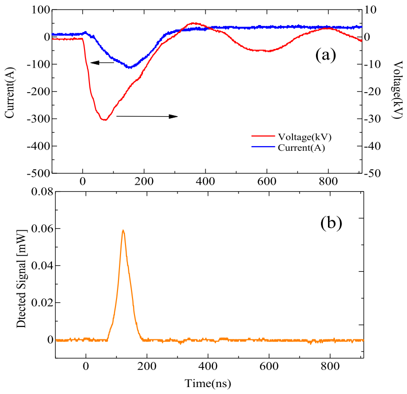

Fig. 6 Waveforms of the measured signals; (a) the beam voltage and the beam current, and (b) the detected signal are presented. The peak signal is detected for a beam voltage and beam current of 22 kV and 110 A, respectively. The magnetic field is 0.6 T.

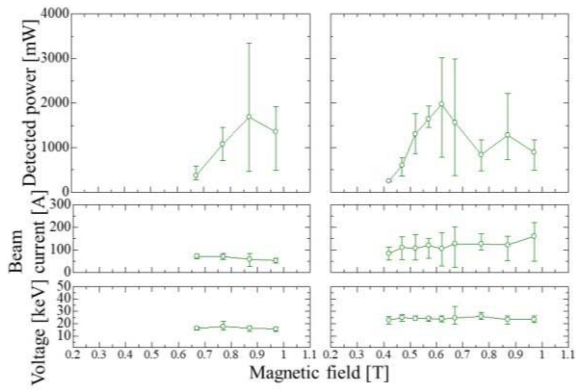

(a) (b)

Fig. 7 Dependence of the F-band SWO operation on the magnetic field (a) for the low beam current and (b) the high beam current.

The maximum value of the detected power is approximately 2000 mW at 0.6 T. The corresponding output power is about 2 kW, which is the same power level as an intense SWO [3]. By increasing the beam current and decreasing the magnetic field, the SC interaction is strengthened and the merged instability occurs, as shown in Fig. 5 (a).

The merged instability may be affected by the distance G_b between the beam and the SWS wall, as well as by the beam current and energy. In Refs. [2, 9], the effective value of G_b was estimated to be 0.125 - 0.05 mm based on the oscillation starting condition for broadband terahertz backward wave oscillators, in which the speed of the surface wave is not so far from the speed of light. In this paper, the surface wave is much slower than the light and concentrates near the SWS wall as shown in Fig. 2 (b). Thus, the effective G_b of the SWO should be reduced. Figure 5 (b) shows the dependence of the EH_{01} instabilities on the magnetic field with $G_b = 0.01$ mm. The beam energy and current are 25 keV and 110 A, respectively, which correspond to the values for intense operation around 0.6 T in Fig. 7 (b). The increased output power in the weak magnetic field region is in fairly good agreement with the occurrence of the merged instability.

5. Discussion and Conclusion

Conventionally, the operation of SWOs has been considered based only on the Cherenkov instability by assuming a sufficiently or infinitely strong magnetic field. However, the magnetic field in real SWO devices may not be strong enough to ignore effects of vertical cyclotron motion. In particular, the SC instability becomes strong and forms a merged instability with the Cherenkov instability at the low magnetic fields. In our experiments, the SWO is able to sustain its power level down to around 0.4 T. This operation agrees well with the merged instability formation owing to the enhanced SC instability. In the magnetic field region less than 0.4 T, poor beam confinement due to the decreased magnetic field might surpass the effect of the large growth rate of the merged instability. For operation with a low beam current, as in Fig. 5 (a), the merged instability may occur at less than 0.3 T, which is too low to intensify the SWO operation.

In conclusion, we examined the F-band SWO operation in the low magnetic field region. By increasing the beam current, the SC instability due to the vertical cyclotron motion is enhanced and forms the merged instability, which is stronger than Cherenkov and SC instabilities and can maintain intense SWO radiation. The merged instability presented in this paper is a very attractive mechanism for developing compact terahertz-wave sources by reducing the size of a magnetic system.

[1] J. Wang *et al.*, Scientific Reports **8**, 6978 (2018).
[2] M.T. San *et al.*, IEEE Plasma Sci. **46**, 530 (2018).
[3] Y. Annaka *et al.*, Jpn. J. Appl. Phys. **59**, SHHD02 (2020).
[4] M.Y. Glyavin *et al.*, Phys. Rev. Lett. **100**, 015101 (2008).
[5] Y. Yamaguchi *et al.*, Plasma Fusion Res. **7**, 1205004 (2012).
[6] K. Ogura *et al.*, IEEE Trans. Plasma Sci. **49**, 40 (2021).
[7] H. Oe *et al.*, J. Plasma Fusion Res. SERIES **8**, 1477 (2009).
[8] O. Watanabe *et al.*, Phys. Rev. E **63**, 056503 (2001).
[9] S. Gong *et al.*, IEEE Plasma Sci. **43**, 3530 (2018).